Ultrasonics 96 (2019) 40–47

Contents lists available at ScienceDirect

Ultrasonics

journal homepage: www.elsevier.com/locate/ultras

A closed-form solution to propagation of guided waves in a layered half-space under a time-harmonic load: An application of elastodynamic reciprocity

Haidang Phan[a,*], Younho Cho[b], Quang Hung Le[c], Chi Vinh Pham[d], Hoai T.-L. Nguyen[e], Phuong Thuy Nguyen[e], Tinh Quoc Bui[f]

[a] Institute of Theoretical and Applied Research, Duy Tan University, 1 Phung Chi Kien, Hanoi 100000, Viet Nam
[b] School of Mechanical Engineering, Pusan National University, Pusan, South Korea
[c] Graduate University of Science and Technology, Vietnam Academy of Science and Technology, Viet Nam
[d] Faculty of Mathematics, Mechanics and Informatics, Hanoi University of Science, Hanoi, Viet Nam
[e] Institute of Physics, Vietnam Academy of Science and Technology, Hanoi, Viet Nam
[f] Department of Civil and Environmental Engineering, Tokyo Institute of Technology, Tokyo, Japan

ARTICLE INFO

Keywords:
Reciprocity
Rayleigh waves
Love waves
Guided waves
Layered half-space

ABSTRACT

This article is concerned with the application of reciprocity in computing guided wave motions generated by a time-harmonic load in a layer of uniform thickness joined to a half-space. Explicit expressions for free Rayleigh waves and Love waves propagating in the layered half-space are introduced. Exact solutions of Rayleigh waves and Love waves are derived from reciprocity relations between an actual state – guided waves generated by a time-harmonic line load and a virtual state – an appropriately chosen free wave traveling in the structure. Scattered amplitudes of the wave motions are thus determined. The validation of the reciprocity approach is shown through the computation of the lowest Rayleigh wave mode in the layered half-space, which approaches the calculation of the Rayleigh surface wave in the half-space once the layer thickness approaches zero in the limit.

1. Introduction

Guided wave propagation in a layer on a half-space can be separated into in-plane Rayleigh waves, also called Rayleigh-Lamb type waves [1] and out-of-plane Love waves. Earlier theoretical modeling works on waves in a layer and a supporting half-space of different material properties can be found, e.g., in textbooks [1–7]. There are also a great number of research articles addressing this interesting topic available in the literature. In particular, dispersion curves for free waves in a layered half-space were analyzed by Achenbach and Keshava [8]. Tiersten [9] investigated the influence of thin film on guided wave propagation in the joined structure of a film over a half-space with comparison to experiment data. Vinh et al. [10] explored the approximate secular equation and the velocity formula for guided wave propagation in an isotropic elastic half-space, which is coated by a thin isotropic elastic layer with smooth contact. In such a way, the approximate secular equations for guided waves in an orthotropic half-space coated by a thin orthotropic layer with sliding contact were also derived and reported in [11] by the same authors.

Reciprocity theorems in general provide a relation between displacements, tractions and body forces for two different loading states of the same body. Statements of elastodynamic reciprocity theorems have already presented, and curious readers can refer to, e.g., Refs. [12–14]. Reciprocity relations have been successfully used in direct applications to compute guided waves generated by a time-harmonic load, see [15–21]. Balogun and Achenbach [15] examined surface waves generated by a line load on a half-space with depth-dependent properties. The applications of reciprocity to surface waves on an inhomogeneous transversely isotropic half-space was discussed by Kulkarni and Achenbach [20]. The reciprocity approach was also applied to study scattering of surface waves by cavities on the surface of a half-space [22–24] and scattering of Lamb waves by a partial spherical corrosion pit in a plate [25].

Due to time-harmonic sources, the elastodynamic reciprocity thus offers a simpler approach for deriving the far-field displacements compared with the conventional integral transform techniques

* Corresponding author.
E-mail address: haidangphan.vn@gmail.com (H. Phan).

https://doi.org/10.1016/j.ultras.2019.03.015
Received 16 October 2018; Received in revised form 15 March 2019; Accepted 16 March 2019
Available online 22 March 2019

reported, for examples, in [3,4,26]. The material to be studied may be anisotropic, inhomogeneous or viscoelastic. The validity of the reciprocity approach was shown by Phan et al. [16,17] for Rayleigh surface waves in a half-space. It was proved that the calculations obtained by the reciprocity consideration and the integral transform techniques are identical. An appropriate theoretical solution of guided waves generated by a time-harmonic load in a layered half-space is, unfortunately, not available in the literature.

In this contribution, our purpose is to apply the reciprocity to compute Rayleigh waves and Love waves due to a time-harmonic source in a layered half-space. Explicit expressions for free guided waves propagating in the layered half-space are proposed in terms of reciprocity theorems. One of the main contributions is the derivation of exact solutions of Rayleigh waves and Love waves due to the load. Moreover, it has been proved one important finding presented in the examples that the obtained computation of the lowest Rayleigh mode in the layered half-space approaches the result of the Rayleigh wave in the half-space once the thickness of the layer approaches zero. The indicated limit is for small layer thickness (i.e. low frequencies).

The rest of the article is divided into five sections. In Section 2, we briefly review the solutions of free Rayleigh waves propagating in a layered half-space and proposes explicit expressions for the displacements and stresses. The reciprocity applications for a layered half-space to obtain the scattered amplitudes of Rayleigh waves generated by a time-harmonic line load are presented in Section 3. The detailed implementation of Love wave motions is given in Section 4, while the calculation of the lowest Rayleigh wave mode is detailed in Section 5. Some major conclusions drawn from this study are given in Section 6.

2. Explicit expressions for Rayleigh waves in a layer half-space

Guided waves may exist in a layer on a half-space in which the materials of the layer and the half-space are different. Let us consider a solid layer Ω and a solid half-space $\widehat{\Omega}$ which are perfectly bonded together along the plane $z = 0$, relative to the Cartesian coordinate system (x, z), see Fig. 1. The Lame constants and mass density of these two materials are indicated by λ, μ, ρ and $\widehat{\lambda}$, $\widehat{\mu}$, $\widehat{\rho}$, respectively, and the thickness of the layer is noted by h. For an isotropic elastic medium, the partial waves polarized in the (x, z) plane can be completely separated from the partial waves polarized in the y−direction. The former is called Rayleigh waves, also Rayleigh-Lamb type waves [1], which is discussed in this section, while the latter is Love waves. The governing equations for a homogeneous isotropic elastic solid are the displacement equations of motion in the absence of body forces [3]

$$\mu u_{i,jj} + (\lambda + \mu)u_{j,ji} = \rho\ddot{u}_i \tag{1}$$

The solutions of Rayleigh waves in a layered half-space can be expressed as a combination of partial waves based on the partial wave theory, which is discussed in detail, for example, in [1]. In this case, there are four partial waves in the layer and two in the half-space.

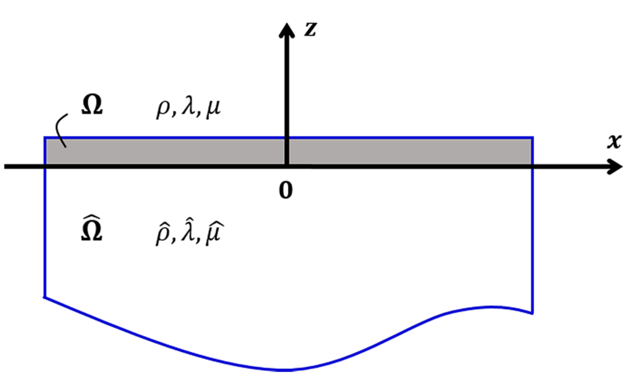

Fig. 1. Coordinate system for guided waves in a layer half-space.

Therefore, the displacements of the layer may be written as

$$u_x = (A_1 e^{ik\alpha_1 z} + A_2 e^{ik\alpha_2 z} + A_3 e^{-ik\alpha_1 z} + A_4 e^{-ik\alpha_2 z})e^{ik(x-ct)} \tag{2}$$

$$u_z = \left(\frac{-1}{\alpha_1}A_1 e^{ik\alpha_1 z} + \alpha_2 A_2 e^{ik\alpha_2 z} + \frac{1}{\alpha_1}A_3 e^{-ik\alpha_1 z} - \alpha_2 A_4 e^{-ik\alpha_2 z}\right)e^{ik(x-ct)} \tag{3}$$

and the displacements of the half-space are of the form

$$\widehat{u}_x = (\widehat{A}_1 e^{k\widehat{\alpha}_1 z} + \widehat{A}_2 e^{k\widehat{\alpha}_2 z})e^{ik(x-ct)} \tag{4}$$

$$\widehat{u}_z = -i\left(\frac{1}{\widehat{\alpha}_1}\widehat{A}_1 e^{k\widehat{\alpha}_1 z} + \widehat{\alpha}_2\widehat{A}_2 e^{k\widehat{\alpha}_2 z}\right)e^{ik(x-ct)} \tag{5}$$

Here, $A_j\,(j = 1, 2, 3, 4)$ and $\widehat{A}_j\,(j = 1, 2)$ are the constants to be determined and $k$indicates the wavenumber where $k = \omega/c$ with ω being the angular frequency and c being the phase velocity.

The dimensionless quantities in Eqs. (2)–(5) are defined in the following.

$$\alpha_1 = \sqrt{-1 + c^2/c_T^2}\ \alpha_2 = \sqrt{-1 + c^2/c_L^2} \tag{6}$$

where

$$c_T = \sqrt{\mu/\rho}\ c_L = \sqrt{(\lambda + 2\mu)/\rho} \tag{7}$$

are the transverse and longitudinal wave velocities, respectively, of the solid layer Ω.

$$\widehat{\alpha}_1 = \sqrt{1 - c^2/\widehat{c}_T^2}\ \widehat{\alpha}_2 = \sqrt{1 - c^2/\widehat{c}_L^2} \tag{8}$$

where

$$\widehat{c}_T = \sqrt{\widehat{\mu}/\widehat{\rho}}\ \widehat{c}_L = \sqrt{(\widehat{\lambda} + 2\widehat{\mu})/\widehat{\rho}} \tag{9}$$

are the transverse and longitudinal wave velocities, respectively, of the half-space $\widehat{\Omega}$. Note that stress components τ_{xx}, τ_{xz}, τ_{zz} of the layer Ω and $\widehat{\tau}_{xx}$, $\widehat{\tau}_{xz}$, $\widehat{\tau}_{zz}$ of the half-space $\widehat{\Omega}$ can be easily calculated from the displacements by the use of Hooke's law.

For Rayleigh waves in this layered half-space, there are two free boundary conditions at the surface $(z = h)$ and four at the interface $(z = 0)$ written as

$$\tau_{xz} = 0, \quad \tau_{zz} = 0\ at\ z = h \tag{10}$$

$$u_x = \widehat{u}_x, \quad u_z = \widehat{u}_z, \quad \tau_{xz} = \widehat{\tau}_{xz}, \quad \tau_{zz} = \widehat{\tau}_{zz}\ at\ z = 0 \tag{11}$$

Eqs. (10) and (11) result in

$$\mathbf{DA} = \mathbf{0} \tag{12}$$

where

$$\mathbf{A} = [A_1\ \ A_2\ \ A_3\ \ A_4\ \ \widehat{A}_1\ \ \widehat{A}_2]^T \tag{13}$$

and $\mathbf{D}$ is the six-by-six matrix whose expression is given in the Appendix, see Eq. (A.1).

To have nontrivial solutions, the determinant of $\mathbf{D}$ in Eq. (12) must be zero. This leads to a transcendental equation with phase velocity as an unknown parameter when the properties of the two materials and the frequency are given. Since the determinant appears with a frequency term via wavenumber k, the phase velocity of Rayleigh wave problems is dependent of frequency. Therefore, Rayleigh waves are dispersive. A numerical method can be used to solve the characteristic equation which results in the dispersion curves.

As an example of calculation, the dispersion curves of a plexiglas layer joined to an aluminum half-space with the material properties tabulated in Table 1 are shown in Fig. 2. It can be seen that the lower bound of the phase velocity value is the Rayleigh wave velocity in the plexiglas while its upper limit value is the shear wave velocity in the aluminum. Also, the wave velocity approaches the Rayleigh surface wave in aluminum at the low frequency limit where the layer thickness is much smaller than the wavelength.

Since the determinant of $\mathbf{D}$ must be zero, Eq. (12) has actually five

Table 1
Material properties of plexiglas and aluminum.

Material	ρ (kg/m^3)	λ (GPa)	μ (GPa)
Plexiglas	1 180	5.45	1.48
Aluminum	2 700	55.25	25.94

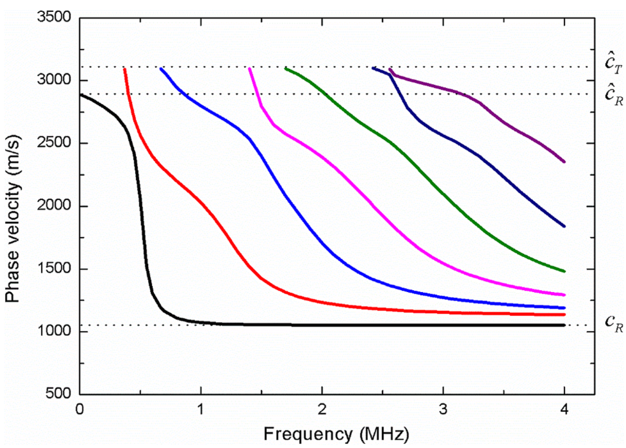

Fig. 2. Dispersion curves for a plexiglas layer of 1 mm thickness and an aluminum half-space – Rayleigh waves.

independent equations with six unknowns $A_1,\ A_2,\ A_3,\ A_4,\ \widehat{A}_1,\ \widehat{A}_2$. It has an infinite number of solutions. A general solution of Eq. (12) is found in the form of

$$A_1 = Ad_1, A_2 = Ad_2, A_3 = Ad_3, A_4 = Ad_4, \widehat{A}_1 = A\widehat{d}_1, \widehat{A}_2 = A\widehat{d}_2 \tag{14}$$

where $A \neq 0$ is an arbitrary constant with a dimension of length while dimensionless quantities $d_1,\ d_2,\ d_3,\ d_4,\ \widehat{d}_1,\ \widehat{d}_2$ depend only on material properties of the layer and the half-space. The equation-solving process to obtain these quantities is quite tedious. Therefore, we provide their expressions without a detailed proof, see Eqs. (A.2)–(A.7).

The displacements and stresses of free Rayleigh waves in a layered half-space may now be rewritten as

$$u_x = AU_x(z)e^{ik(x-ct)} \tag{15}$$

$$u_z = AU_z(z)e^{ik(x-ct)} \tag{16}$$

$$\tau_{xx} = ik\mu AT_{xx}(z)e^{ik(x-ct)} \tag{17}$$

$$\tau_{xz} = ik\mu AT_{xz}(z)e^{ik(x-ct)} \tag{18}$$

where

$$U_x(z) = d_1e^{ik\alpha_1 z} + d_2e^{ik\alpha_2 z} + d_3e^{-ik\alpha_1 z} + d_4e^{-ik\alpha_2 z} \tag{19}$$

$$U_z(z) = \frac{-1}{\alpha_1}d_1e^{ik\alpha_1 z} + \alpha_2d_2e^{ik\alpha_2 z} + \frac{1}{\alpha_1}d_3e^{-ik\alpha_1 z} - \alpha_2d_4e^{-ik\alpha_2 z} \tag{20}$$

$$T_{xx}(z) = 2d_1e^{ik\alpha_1 z} + (\alpha_1^2 - 2\alpha_2^2 + 1)d_2e^{ik\alpha_2 z} + 2d_3e^{-ik\alpha_1 z} + (\alpha_1^2 - 2\alpha_2^2 + 1)d_4e^{-ik\alpha_2 z} \tag{21}$$

$$T_{xz}(z) = \left(\alpha_1 - \frac{1}{\alpha_1}\right)d_1e^{ik\alpha_1 z} + 2\alpha_2d_2e^{ik\alpha_2 z} - \left(\alpha_1 - \frac{1}{\alpha_1}\right)d_3e^{-ik\alpha_1 z} - 2\alpha_2d_4e^{-ik\alpha_2 z} \tag{22}$$

for material Ω. For material $\widehat{\Omega}$ they are

$$\hat{u}_x = A\widehat{U}_x(z)e^{ik(x-ct)} \tag{23}$$

$$\hat{u}_z = -iA\widehat{U}_z(z)e^{ik(x-ct)} \tag{24}$$

$$\hat{\tau}_{xx} = ik\hat{\mu}A\widehat{T}_{xx}(z)e^{ik(x-ct)} \tag{25}$$

$$\hat{\tau}_{xz} = k\hat{\mu}A\widehat{T}_{xz}(z)e^{ik(x-ct)} \tag{26}$$

where

$$\widehat{U}_x(z) = \widehat{d}_1e^{k\widehat{\alpha}_1 z} + \widehat{d}_2e^{k\widehat{\alpha}_2 z} \tag{27}$$

$$\widehat{U}_z(z) = \frac{1}{\widehat{\alpha}_1}\widehat{d}_1e^{k\widehat{\alpha}_1 z} + \widehat{\alpha}_2\widehat{d}_2e^{k\widehat{\alpha}_2 z} \tag{28}$$

$$\widehat{T}_{xx}(z) = 2\widehat{d}_1e^{k\widehat{\alpha}_1 z} + (2\widehat{\alpha}_2^2 - \widehat{\alpha}_1^2 + 1)\widehat{d}_2e^{k\widehat{\alpha}_2 z} \tag{29}$$

$$\widehat{T}_{xz}(z) = \left(\widehat{\alpha}_1 + \frac{1}{\widehat{\alpha}_1}\right)\widehat{d}_1e^{k\widehat{\alpha}_1 z} + 2\widehat{\alpha}_2\widehat{d}_2e^{k\widehat{\alpha}_2 z} \tag{30}$$

Here, $U_x(z),\ U_z(z),\ T_{xx}(z),\ T_{xz}(z)$ and $\widehat{U}_x(z),\ \widehat{U}_z(z),\ \widehat{T}_{xx}(z),\ \widehat{T}_{xz}(z)$ are functions of depth z. They are all dimensionless quantities as well as $d_1,\ d_2,\ d_3,\ d_4,\ \widehat{d}_1,\ \widehat{d}_2$ which are dependent on the material properties of the layer and the half-space. In Eqs. (15)–(18) and (23)–(26), there is only one unknown constant A, which we refer to as the relative amplitude of Rayleigh waves in a layered half-space, to be computed by reciprocity considerations in the next section.

3. Computation of Rayleigh wave motions by reciprocity considerations

Reciprocity theorems, in general, offer a relation between displacements, tractions and body forces for two different loading states of an elastic body. As will be discussed, it is possible to use the reciprocity relations to obtain closed-form solution of Rayleigh waves generated by a time-harmonic load in a layered half-space. The reciprocity theorem for a two-material body was studied in [12,19] written as

$$\int_{\Omega} (f_j^A u_j^B - f_j^B u_j^A)d\Omega + \int_{\widehat{\Omega}} (\widehat{f}_j^A \hat{u}_j^B - \widehat{f}_j^B \hat{u}_j^A)d\widehat{\Omega} = \int_S (\tau_{ij}^B u_j^A - \tau_{ij}^A u_j^B)n_i dS + \int_{\widehat{S}} (\hat{\tau}_{ij}^B \hat{u}_j^A - \hat{\tau}_{ij}^A \hat{u}_j^B)\hat{n}_i d\widehat{S} \tag{31}$$

Here, S and $\widehat{S}$ defines contours around domains Ω and $\widehat{\Omega}$ without the interface, respectively, while n_i and $\hat{n}_i$ are normal vectors, see Fig. 3. Superscripts A and B denote two elastodynamic states. For the computation discussed in this section, state A, the actual state, is the field generated by a time-harmonic loading while state B, the virtual state, is the field of a free Rayleigh wave in the layered half-space.

We first consider a vertical load applied at $(x_0,\ z_0)$ where $x_0,\ \ z_0$ are the x−coordinate and the z−coordinate, respectively, of the point of application, see Fig. 3. The load is of the form

$$f_z^A = P\delta(z - z_0)\delta(x - x_0)e^{-ikct} \tag{32}$$

The load generates both propagating and evanescent wave modes in the layered half-space. Real-valued wavenumbers correspond to propagating modes while imaginary and complex wavenumbers correspond to evanescent modes. The amplitude of the evanescent wave modes decays exponentially with respect to x, around or less than a wavelength of a propagating mode at the same frequency [1]. Only the

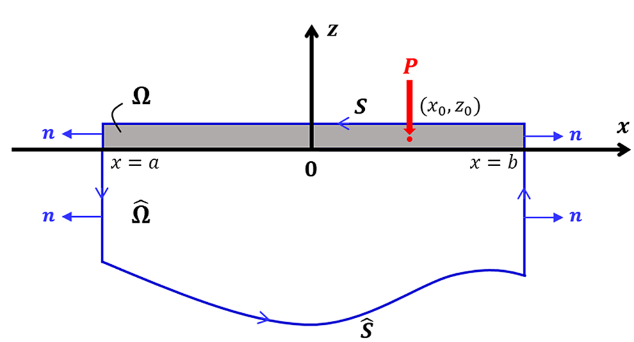

Fig. 3. Layered half-space subjected to a time-harmonic load.

propagating modes are therefore of critical interest for purposes of nondestructive evaluation and structural health monitoring.

For the propagating modes, since the body waves suffer a geometrical attenuation while the Rayleigh waves are not geometrically attenuated, the Rayleigh wave modes dominate in the far field. The wave motion can then be expressed as a summation over the Rayleigh wave modes. The expansions for the far-field displacements of the actual state A in the positive $x-$direction ($x > 0$) may be written as

$$u_x = \sum_{m=0}^{\infty} u_x^m = \sum_{m=0}^{\infty} A_m^{P+} U_x^m(z) e^{ik_m(x-c_m t)} \tag{33}$$

$$u_z = \sum_{m=0}^{\infty} u_z^m = \sum_{m=0}^{\infty} A_m^{P+} U_z^m(z) e^{ik_m(x-c_m t)} \tag{34}$$

and

$$\hat{u}_x = \sum_{m=0}^{\infty} \hat{u}_x^m = \sum_{m=0}^{\infty} A_m^{P+} \hat{U}_x^m(z) e^{ik_m(x-c_m t)} \tag{35}$$

$$\hat{u}_z = \sum_{m=0}^{\infty} \hat{u}_z^m = -i \sum_{m=0}^{\infty} A_m^{P+} \hat{U}_z^m(z) e^{ik_m(x-c_m t)} \tag{36}$$

where A_m^{P+} are unknown relative scattered amplitudes of mode m. For a given frequency, the wavenumber k_m follows from the characteristic equation. The functions $U_x^m(z)$, $U_z^m(z)$ and $\hat{U}_x^m(z)$, $\hat{U}_z^m(z)$ are defined by Eqs. (19,20) and Eqs. (27,28), respectively. Similar expansions can be written for the stress components but they are skipped here for brevity. Note that although the summations are for an infinite number of modes, the actual number is finite since only modes with real-valued wavenumbers are included.

The virtual wave of mode n, state B, is first chosen in the negative $x-$direction

$$u_x^n = -B_n U_x^n(z) e^{-ik_n(x+c_n t)} \tag{37}$$

$$u_z^n = B_n U_z^n(z) e^{-ik_n(x+c_n t)} \tag{38}$$

and

$$\hat{u}_x^n = -B_n \hat{U}_x^n(z) e^{-ik_n(x+c_n t)} \tag{39}$$

$$\hat{u}_z^n = -iB_n \hat{U}_z^n(z) e^{-ik_n(x+c_n t)} \tag{40}$$

Application of the reciprocity relation is now considered over a domain defined by $a \leqslant x \leqslant b$, $-\infty < z \leqslant h$ (Fig. 3). There is no contribution of the integral along to the top surface of the layered half-space since a free boundary condition is applied. Moreover, the contribution from the integration along the line at constant z is not included since it vanishes as $z \to -\infty$. Therefore, Eq. (31) can be reduced as

$$Pu_z^{Bn}(x_0, z_0) e^{-ik_n c_n t} = \sum_{m=0}^{\infty} \left(-\int_0^h F_{AB}^{mn}|_{x=a} dz - \int_{-\infty}^0 \hat{F}_{AB}^{mn}|_{x=a} dz + \int_0^h F_{AB}^{mn}|_{x=b} dz + \int_{-\infty}^0 \hat{F}_{AB}^{mn}|_{x=b} dz \right) \tag{41}$$

where

$$F_{AB}^{mn} = \tau_{xx}^{Bn} u_x^{Am} + \tau_{xz}^{Bn} u_z^{Am} - \tau_{xx}^{Am} u_x^{Bn} - \tau_{xz}^{Am} u_z^{Bn} \tag{42}$$

$$\hat{F}_{AB}^{mn} = \hat{\tau}_{xx}^{Bn} \hat{u}_x^{Am} + \hat{\tau}_{xz}^{Bn} \hat{u}_z^{Am} - \hat{\tau}_{xx}^{Am} \hat{u}_x^{Bn} - \hat{\tau}_{xz}^{Am} \hat{u}_z^{Bn} \tag{43}$$

It can be easily shown that the integration along $x = a$ and $x = b$ in Eq. (41) only yield contributions from counter-propagating waves. For state B in the negative $x-$direction, there is only contribution along $x = b$. Eq. (41) becomes

$$PB_n U_z^n(z_0) e^{-ik_n x_0} e^{-2ik_n c_n t} = \sum_{m=0}^{\infty} \left(\int_0^h F_{AB}^{mn}|_{x=b} dz + \int_{-\infty}^0 \hat{F}_{AB}^{mn}|_{x=b} dz \right) \tag{44}$$

Substitution of the expressions of displacements and stresses of the states A and B into Eq. (44), after some manipulation, leads to

$$PU_z^n(z_0) e^{-ik_n x_0} = \sum_{m=0}^{\infty} 2A_m^{P+} e^{i(k_m-k_n)b} (\mu I_{mn} + \hat{\mu} \hat{I}_{mn}) \tag{45}$$

where

$$I_{mn} = \frac{1}{2} \int_0^h i[k_n(T_{xx}^n(z) U_x^m(z) - T_{xz}^n(z) U_z^m(z)) + k_m(T_{xx}^m(z) U_x^n(z) - T_{xz}^m(z) U_z^n(z))] dz \tag{46}$$

$$\hat{I}_{mn} = \frac{1}{2} \int_{-\infty}^0 i[k_n(\hat{T}_{xx}^n(z) \hat{U}_x^m(z) + \hat{T}_{xz}^n(z) \hat{U}_z^m(z)) + k_m(\hat{T}_{xx}^m(z) \hat{U}_x^n(z) + \hat{T}_{xz}^m(z) \hat{U}_z^n(z))] dz \tag{47}$$

By the use of the orthogonality relation for counter-propagating Rayleigh modes see Eq. (B.4) of the Appendix B for detail, the right-hand side of Eq. (45) cancels out for $m \neq n$. Thus

$$A_n^{P+} = \frac{PU_z^n(z_0) e^{-ik_n x_0}}{2(\mu I_{nn} + \hat{\mu} \hat{I}_{nn})} \tag{48}$$

where

$$I_{nn} = ik_n \int_0^h [T_{xx}^n(z) U_x^n(z) - T_{xz}^n(z) U_z^n(z)] dz \tag{49}$$

$$\hat{I}_{nn} = ik_n \int_{-\infty}^0 [\hat{T}_{xx}^n(z) \hat{U}_x^n(z) + \hat{T}_{xz}^n(z) \hat{U}_z^n(z)] dz \tag{50}$$

with $U_x^n(z)$, $U_z^n(z)$, $T_{xx}^n(z)$, $T_{xz}^n(z)$ and $\hat{U}_x^n(z)$, $\hat{U}_z^n(z)$, $\hat{T}_{xx}^n(z)$, $\hat{T}_{xz}^n(z)$ following from Eqs. (19)–(22) and Eqs. (27)–(30) for the given wavenumber k_n of mode n, respectively. Detailed calculations of I_{nn}, $\hat{I}_{nn}$ are shown in the Appendix C, see Eqs. (C.1)–(C.6).

For virtual state B chosen in the positive $x-$direction, there is only contribution of the integration along $x = a$ in Eq. (41)

$$PB_n U_z^n(z_0) e^{ik_n x_0} e^{-2ik_n c_n t} = \sum_{m=0}^{\infty} \left(-\int_0^h F_{AB}^{mn}|_{x=a} dz - \int_{-\infty}^0 \hat{F}_{AB}^{mn}|_{x=a} dz \right) \tag{51}$$

which becomes

$$PU_z^n(z_0) e^{ik_n x_0} = \sum_{m=0}^{\infty} 2A_m^{P-} e^{i(k_m-k_n)a} (\mu I_{mn} + \hat{\mu} \hat{I}_{mn}) \tag{52}$$

The orthogonality condition is again applied to find the scattered amplitude in the negative direction due to the vertical load

$$A_n^{P-} = \frac{PU_z^n(z_0) e^{ik_n x_0}}{2(\mu I_n + \hat{\mu} \hat{I}_n)} \tag{53}$$

which is equal to A_n^{P+} of Eq. (48) in magnitude.

Consider now is the Rayleigh wave motions generated by a time-harmonic horizontal load, which is of the form

$$f_x^A = Q\delta(z - z_0)\delta(x - x_0) e^{-ikct} \tag{54}$$

Similarly, the load will generate Rayleigh waves along the structure in both the positive and negative $x-$directions with unknown relative scattered amplitudes A_Q^{m+} and A_Q^{m-}, respectively, where $m = 0, 1, \ldots, \infty$ indicate modes. Consider state B, the virtual wave of mode n in the negative direction. Following the same procedure as the case of the vertical load, Eq. (44) is now of the form

$$-QB_n U_x^n(z_0) e^{-ik_n x_0} e^{-2ik_n c_n t} = \sum_{m=0}^{\infty} \left(\int_0^h F_{AB}^{mn}|_{x=b} dz + \int_{-\infty}^0 \hat{F}_{AB}^{mn}|_{x=b} dz \right) \tag{55}$$

It yields the scattered amplitude in the positive direction due to the horizontal load

$$A_n^{Q+} = \frac{-QU_x^n(z_0)e^{-ik_nx_0}}{2(\mu I_n + \hat{\mu}\hat{I}_n)} \tag{56}$$

Scattered amplitude in the negative x−direction can be found in a similar manner as

$$A_n^{Q-} = \frac{QU_x^n(z_0)e^{ik_nx_0}}{2(\mu I_n + \hat{\mu}\hat{I}_n)} \tag{57}$$

It should be noted that A_n^{Q+} is equal to A_n^{Q-} in magnitude.

4. Reciprocity approach for Love wave motions

The guided wave modes polarized in the y−direction in a layered half-space (Fig. 1) are called Love waves. The displacements of the layer and the half-space can be rewritten as

$$u_y = (A_1e^{ik\beta z} + A_2e^{-ik\beta z})e^{ik(x-ct)} \tag{58}$$

$$\hat{u}_y = \hat{A}_1e^{k\hat{\beta}z}e^{ik(x-ct)} \tag{59}$$

where A_1, A_2 and $\hat{A}_1$ are constants to be determined. The dimensionless quantities in Eqs. (58,59) are defined as

$$\beta = \sqrt{-1 + c^2/c_T^2} \tag{60}$$

$$\hat{\beta} = \sqrt{1 - c^2/\hat{c}_T^2} \tag{61}$$

where $c_T = \sqrt{\mu/\rho}$ and $\hat{c}_T = \sqrt{\hat{\mu}/\hat{\rho}}$ are the transverse wave velocities of the layer Ω and the half-space $\hat{\Omega}$, respectively.

There one free boundary condition at the surface ($z = h$) and two boundary conditions at the interface ($z = 0$) which are written as

$$u_y = \hat{u}_y, \quad \tau_{yz} = \hat{\tau}_{yz} \text{ at } z = 0 \tag{62}$$

$$\tau_{yz} = 0 \text{ at } = h \tag{63}$$

Eqs. (62) and (63) result in a system of three equations

$$\begin{bmatrix} e^{ik\hat{\beta}h} & -e^{-ik\hat{\beta}h} & 0 \\ 1 & 1 & -1 \\ \hat{\beta} & -\hat{\beta} & i\mu_0\hat{\beta} \end{bmatrix} \begin{bmatrix} A_1 \\ A_2 \\ \hat{A}_1 \end{bmatrix} = \mathbf{0} \tag{64}$$

where $\mu_0 = \hat{\mu}/\mu$. The determinant of the three-by-three matrix in Eq. (64) must be zero for nontrivial solutions. This will lead to an equation with phase velocity as an unknown parameter when the properties of the two materials and the frequency are given. Since the determinant appears with a frequency term via wavenumber k, Love wave is also dispersive. Love wave dispersion curves of a plexiglas layer joined to an aluminum half-space with material properties tabulated in Table 1 are displayed in Fig. 4.

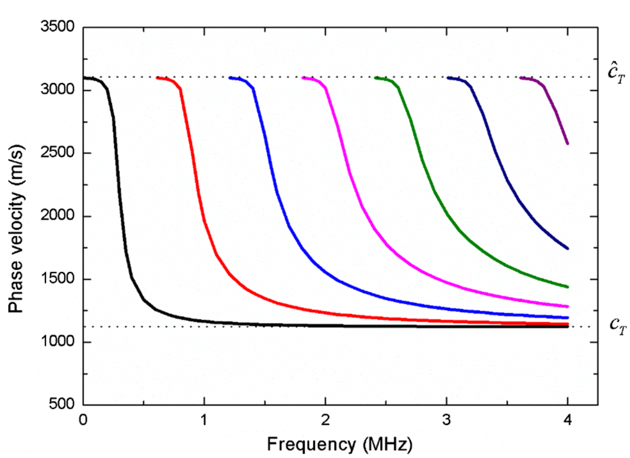

Fig. 4. Dispersion curves for a plexiglas layer of 1 mm thickness and an aluminum half-space – Love waves.

As the determinant of the matrix is zero, Eq. (64) has actually two independent equations with three unknowns A_1, A_2, $\hat{A}_1$; thus, it has an infinite number of solutions. A general solution may be found in the form of

$$A_1 = Ad_1, A_2 = Ad_2, \hat{A}_1 = A\hat{d}_1 \tag{65}$$

where $A \neq 0$ is an arbitrary constant which has a dimension of length while dimensionless quantities d_1, d_2, $\hat{d}_1$ depend only on material properties of the layer and the half-space. Expressions of d_1, d_2, $\hat{d}_1$ can be found as

$$d_1 = \beta - i\mu_0\hat{\beta} \; d_2 = \beta + i\mu_0\hat{\beta} \; \hat{d}_1 = 2\beta \tag{66}$$

The displacements and stress components can now be rewritten as

$$u_y = AU_y(z)e^{ik(x-ct)} \tag{67}$$

$$\tau_{xy} = ik\mu AU_y(z)e^{ik(x-ct)} \tag{68}$$

where

$$U_y(z) = d_1e^{ik\beta z} + d_2e^{-ik\beta z} \tag{69}$$

and

$$\hat{u}_y = A\hat{U}_y(z)e^{ik(x-ct)} \tag{70}$$

$$\hat{\tau}_{xy} = ik\hat{\mu}A\hat{U}_y(z)e^{ik(x-ct)} \tag{71}$$

where

$$\hat{U}_y(z) = \hat{d}_1e^{k\hat{\beta}z} \tag{72}$$

In Eqs. (67,68) and (70,71), again, there is only one unknown constant A, which we refer to as the relative amplitude, to be determined by the use of reciprocity theorems.

Love wave motions radiated by a time-harmonic line load are now calculated by reciprocity considerations. This study is considered for a horizontal time-harmonic load in the y−direction applied at (x_0, z_0) where x_0, z_0 are the x−coordinate and the z−coordinate, respectively, of the point of application. The load is of the form

$$f_y^A = R\delta(z - z_0)\delta(x - x_0)e^{-ikct} \tag{73}$$

Love waves will be generated along the structure in both the positive and negative x−directions with unknown relative scattered amplitudes A_m^{R+} and A_m^{R-}, respectively, where $m = 0, 1, ..., \infty$ indicate the mode. This is the actual state A whose amplitudes are to be determined. The expansions for the far-field displacements and the stresses of state A in the positive direction ($x > 0$) may be written as

$$u_y = \sum_{m=0}^{\infty} u_y^m = \sum_{m=0}^{\infty} A_m^{R+}U_y^m(z)e^{ik_m(x-c_mt)} \tag{74}$$

$$\hat{u}_y = \sum_{m=0}^{\infty} \hat{u}_y^m = \sum_{m=0}^{\infty} A_m^{R+}\hat{U}_y^m(z)e^{ik_m(x-c_mt)} \tag{75}$$

State B in the negative x−direction, a free Love wave of mode n, may be expressed as

$$u_y^n = B_nU_y^n(z)e^{-ik_n(x+c_nt)} \tag{76}$$

$$\hat{u}_y^n = B_n\hat{U}_y^n(z)e^{-ik_n(x+c_nt)} \tag{77}$$

The reciprocity relation in Eq. (31) is again used for the calculation of Love wave motions. Eq. (44) for virtual state B in the negative x−direction is now of the form

$$RB_nU_y^n(z_0)e^{-ik_nx_0}e^{-2ik_nc_nt} = \sum_{m=0}^{\infty}\left(\int_0^h H_{AB}^{nn}|_{x=b}dz + \int_{-\infty}^0 \hat{H}_{AB}^{nn}|_{x=b}dz\right) \tag{78}$$

An orthogonality condition can be easily derived for Love waves in a layered half-space. For this condition, we finally obtain

$$A_n^{R+} = \frac{RU_y^n(z_0)e^{-ik_n x_0}}{2(\mu L_n + \hat{\mu}\hat{L}_n)} \tag{79}$$

where L_n, $\hat{L}_n$ are dimensionless quantities which can be calculated as

$$L = \frac{-d_1^2}{2\beta}(e^{2ik\beta h} - 1) + \frac{d_2^2}{2\beta}(e^{-2ik\beta h} - 1) - 2ikhd_1d_2 \tag{80}$$

$$\hat{L} = \frac{-i\hat{d}_1^2}{2\hat{\beta}} \tag{81}$$

Similarly, we find the scattered amplitude in the negative x−direction due to the horizontal load

$$A_n^{R-} = \frac{RU_y^n(z_0)e^{-ik_n x_0}}{2(\mu L_n + \hat{\mu}\hat{L}_n)} \tag{82}$$

5. Example: calculation of the lowest Rayleigh wave mode

The low modes of Rayleigh waves are very useful for application in nondestructive evaluation. In this section, we consider computation of the lowest Rayleigh mode in a plexiglas layer joined to an aluminum half-space. Their material properties are given in Table 1. As shown in Fig. 2 that only the lowest Rayleigh mode exists in the layered half-space as $f \leqslant 0.3$ MHz or $fh \leqslant 0.3$ (MHz·mm). When the thickness of the plexiglas layer is much smaller than the wavelength, the phase velocity approaches the velocity of Rayleigh surface wave in the aluminum half-space. As a consequence, the influence of the layer on wave propagation is very small.

It is now of interest to show that the displacement amplitudes of the lowest Rayleigh wave mode approach the amplitudes of Rayleigh waves as the thickness of the layer h approaches zero in the limit for a fixed finite values of frequency f. It means that fh goes to zero. The frequency is $f = 1$ MHz while the thickness of the layer varies from $h = 0$ to $h = 0.3$ mm. The vertical and horizontal loads are applied on the free surface of layer with the magnitude chosen as $P = Q = \hat{\mu}/2$. The loads generate the lowest Rayleigh wave modes with scattered amplitudes A_0^P and A_0^Q, respectively. These amplitudes are compared with the ones of surface waves in an aluminum half-space, A_R^P and A_R^Q, obtained by Phan et al. [16]. The amplitude ratios of the lowest Rayleigh mode to the Rayleigh wave, A_0^P/A_R^P due to vertical load P and A_0^Q/A_R^Q due to horizontal load Q, are visualized in Figs. 5 and 6, respectively. It can be easily seen that $A_0^P/A_R^P \to 1$ and $A_0^Q/A_R^Q \to 1$ as the thickness of the layer approaches to zero. This indicates the validation of the reciprocity approach discussed in the current study.

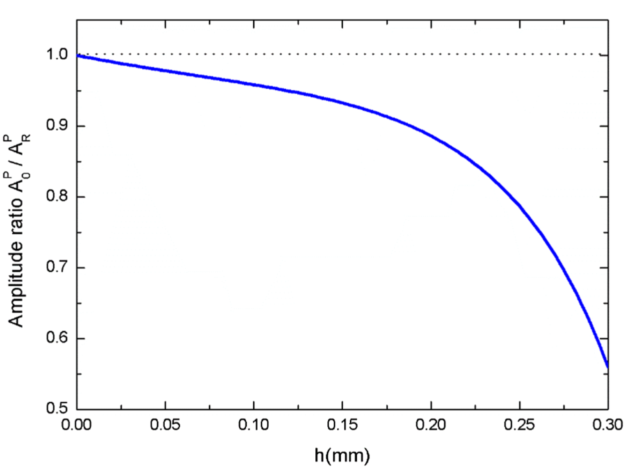

Fig. 5. Amplitude ratio of lowest Rayleigh mode in the layered half-space to Rayleigh wave in the half-space due to vertical loading.

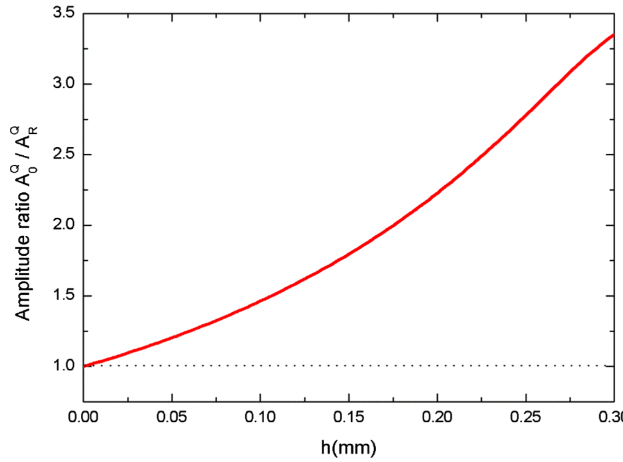

Fig. 6. Amplitude ratio of lowest Rayleigh mode in the layered half-space to Rayleigh wave in the half-space due to horizontal loading.

6. Conclusions

In this paper, we have theoretically analyzed the motions of Rayleigh waves and Love waves generated by a time-harmonic source in an elastic layer of uniform thickness joined to an elastic half-space. We have introduced explicit expressions of free Rayleigh type waves in order to perform direct applications of the reciprocity relations. One of the main contributions of this work is the derivation of exact solutions of Rayleigh waves and Love waves due to the load. Also, it has been proved one important finding as shown in the examples that the obtained calculation of the lowest Rayleigh mode in the layered half-space approaches the computation of the Rayleigh wave in the half-space as the thickness of the layer approaches zero in the limit. This demonstrates the validation of the reciprocity approach presented in the current investigation. The obtained results and expressions reported in this study could be, in general, useful for the applications and development in the area of nondestructive evaluation and structural health monitoring.

Acknowledgement

This research is funded by Graduate University of Science and Technology under grant number GUST.STS.ĐT2017-CH01; and Vietnam National Foundation for Science and Technology Development (NAFOSTED) under grant number 107.02-2016.23.

Appendix A:. Expressions of free Rayleigh waves in a layered half-space

$$\mathbf{D}=\begin{bmatrix}(\alpha_1-\alpha_1^{-1})e^{ik\alpha_1h} & 2\alpha_2e^{ik\alpha_2h} & (\alpha_1^{-1}-\alpha_1)e^{-ik\alpha_1h} & -2\alpha_2e^{-ik\alpha_2h} & 0 & 0\\ -2e^{ik\alpha_1h} & (\alpha_1^2-1)e^{ik\alpha_2h} & -2e^{-ik\alpha_1h} & (\alpha_1^2-1)e^{-ik\alpha_2h} & 0 & 0\\ 1 & 1 & 1 & 1 & -1 & -1\\ -\alpha_1^{-1} & \alpha_2 & \alpha_1^{-1} & -\alpha_2 & i\hat{\alpha}_1^{-1} & i\hat{\alpha}_2\\ \alpha_1-\alpha_1^{-1} & 2\alpha_2 & \alpha_1^{-1}-\alpha_1 & -2\alpha_2 & i\mu_0(\hat{\alpha}_1+\hat{\alpha}_1^{-1}) & 2i\mu_0\hat{\alpha}_2\\ -2 & \alpha_1^2-1 & -2 & \alpha_1^2-1 & 2\mu_0 & \mu_0(\hat{\alpha}_1^2+1)\end{bmatrix} \tag{A.1}$$

where $\mu_0=\hat{\mu}/\mu$.

$$d_1=\frac{[\hat{\alpha}_1(\alpha_1^2-1+2\mu_0)+i\alpha_1(2-\mu_0-\mu_0\hat{\alpha}_1^2)]\hat{d}_1+[\hat{\alpha}_1(\alpha_1^2-1+\mu_0+\mu_0\hat{\alpha}_1^2)+2i\alpha_1\hat{\alpha}_1\hat{\alpha}_2(1-\mu_0)]\hat{d}_2}{2\hat{\alpha}_1(\alpha_1^2+1)} \tag{A.2}$$

$$d_2=\frac{[2\hat{\alpha}_1\alpha_2(1-\mu_0)+i(1-\alpha_1^2-\mu_0-\mu_0\hat{\alpha}_1^2)]\hat{d}_1+[\hat{\alpha}_1\alpha_2(2-\mu_0-\mu_0\hat{\alpha}_1^2)+i\hat{\alpha}_1\hat{\alpha}_2(1-\alpha_1^2-2\mu_0)]\hat{d}_2}{2(\alpha_1^2+1)\hat{\alpha}_1\alpha_2} \tag{A.3}$$

$$d_3=\frac{[\hat{\alpha}_1(\alpha_1^2-1+2\mu_0)-i\alpha_1(2-\mu_0-\mu_0\hat{\alpha}_1^2)]\hat{d}_1+[\hat{\alpha}_1(\alpha_1^2-1+\mu_0+\mu_0\hat{\alpha}_1^2)-2i\alpha_1\hat{\alpha}_1\hat{\alpha}_2(1-\mu_0)]\hat{d}_2}{2\hat{\alpha}_1(\alpha_1^2+1)} \tag{A.4}$$

$$d_4=\frac{[\hat{\alpha}_1\alpha_2(2-2\mu_0)-i(1-\alpha_1^2-\mu_0-\mu_0\hat{\alpha}_1^2)]\hat{d}_1+[\hat{\alpha}_1\alpha_2(2-\mu_0-\mu_0\hat{\alpha}_1^2)-i\hat{\alpha}_1\hat{\alpha}_2(1-\alpha_1^2-2\mu_0)]\hat{d}_2}{2(\alpha_1^2+1)\hat{\alpha}_1\alpha_2} \tag{A.5}$$

where

$$\hat{d}_1=\left[2\hat{\alpha}_2(\alpha_1^2-1)(1-\mu_0)\cos k\alpha_1h+\frac{(\alpha_1^2-1)(\alpha_1^2-1+\mu_0+\mu_0\hat{\alpha}_1^2)}{\alpha_1}\sin k\alpha_1h+2\hat{\alpha}_2(1-\alpha_1^2-2\mu_0)\cos k\alpha_2h+2\alpha_2(2-\mu_0-\mu_0\hat{\alpha}_1^2)\sin k\alpha_2h\right] \tag{A.6}$$

$$\hat{d}_2=-\left[\frac{(\alpha_1^2-1)(2-\mu_0-\mu_0\hat{\alpha}_1^2)}{\hat{\alpha}_1}\cos k\alpha_1h+\frac{(\alpha_1^2-1)(\alpha_1^2-1+2\mu_0)}{\alpha_1}\sin k\alpha_1h+\frac{2(1-\alpha_1^2-\mu_0-\mu_0\hat{\alpha}_1^2)}{\hat{\alpha}_1}\cos k\alpha_2h+4\alpha_2(1-\mu_0)\sin k\alpha_2h\right] \tag{A.7}$$

Appendix B:. Orthogonality condition

An orthogonality condition for counter-propagating Rayleigh wave modes in a layered half-space is derived by application of the reciprocity relation in Eq. (31) to two free Rayleigh waves. State A is mode m with wavenumber k_m and state B represents mode n with wavenumber k_n. The domain is defined by $a\leqslant x\leqslant b,\ -\infty<z\leqslant h$, see Fig. 3. Since there is no force term, the left-hand side of Eq. (31) vanishes. Thus

$$\int_S(\tau_{ij}^Bu_j^A-\tau_{ij}^Au_j^B)n_idS+\int_{\hat{S}}(\hat{\tau}_{ij}^B\hat{u}_j^A-\hat{\tau}_{ij}^A\hat{u}_j^B)\hat{n}_id\hat{S}=0 \tag{B.1}$$

We may write

$$\int_0^hF_{AB}^{mn}|_{x=a}dz+\int_{-\infty}^0\hat{F}_{AB}^{mn}|_{x=a}dz=\int_0^hF_{AB}^{mn}|_{x=b}dz+\int_{-\infty}^0\hat{F}_{AB}^{mn}|_{x=b}dz \tag{B.2}$$

where F_{AB}^{mn} and $\hat{F}_{AB}^{mn}$ follow from Eqs. (42,43). Substitution of the expressions of displacements and stresses of the states A and B into Eq. (44), after some manipulation, yields

$$(e^{i(k_m-k_n)a}-e^{i(k_m-k_n)b})(\mu I_{mn}+\hat{\mu}\hat{I}_{mn})=0 \tag{B.3}$$

where I_{mn} and $\hat{I}_{mn}$ are defined by Eqs. (46,47).

Eq. (B.3) must be satisfied for arbitrary values of a and b. It is satisfied for $m=n$. When $m\neq n$, Eq. (B.3) can be satisfied only if $\mu I_{mn}+\hat{\mu}\hat{I}_{mn}=0$. Therefore

$$\mu I_{mn}+\hat{\mu}\hat{I}_{mn}=0\ \text{for}\ m\neq n \tag{B.4}$$

This is the orthogonality condition for Rayleigh waves in a layered half-space.

Appendix C:. Calculation of integrals I, $\hat{I}$

$$I=ik\int_0^h\left[\begin{matrix}(2d_1e^{ik\alpha_1z}+(\alpha_1^2-2\alpha_2^2+1)d_2e^{ik\alpha_2z}+2d_3e^{-ik\alpha_1z}+(\alpha_1^2-2\alpha_2^2+1)d_4e^{-ik\alpha_2z})(d_1e^{ik\alpha_1z}+d_2e^{ik\alpha_2z}+d_3e^{-ik\alpha_1z}+d_4e^{-ik\alpha_2z})-\\((\alpha_1-\alpha_1^{-1})d_1e^{ik\alpha_1z}+2\alpha_2d_2e^{ik\alpha_2z}-(\alpha_1-\alpha_1^{-1})d_3e^{-ik\alpha_1z}-2\alpha_2d_4e^{-ik\alpha_2z})(-\alpha_1^{-1}d_1e^{ik\alpha_1z}+\alpha_2d_2e^{ik\alpha_2z}+\alpha_1^{-1}d_3e^{-ik\alpha_1z}-\alpha_2d_4e^{-ik\alpha_2z})\end{matrix}\right]dz \tag{C.1}$$

$$I=ik\int_0^h\left[\begin{matrix}\left(3-\frac{1}{\alpha_1^2}\right)d_1^2e^{2ik\alpha_1z}+\left(\alpha_1^2-2\alpha_2^2-\alpha_1\alpha_2+\frac{3\alpha_2}{\alpha_1}+3\right)d_1d_2e^{ik(\alpha_1+\alpha_2)z}+\left(2+\frac{2}{\alpha_1^2}\right)d_1d_3+\left(\alpha_1^2-2\alpha_2^2+3+\alpha_1\alpha_2-\frac{3\alpha_2}{\alpha_1}\right)d_1d_4e^{ik(\alpha_1-\alpha_2)z}\\+(\alpha_1^2-4\alpha_2^2+1)d_2^2e^{2ik\alpha_2z}+\left(\alpha_1^2-2\alpha_2^2+3-\frac{3\alpha_2}{\alpha_1}+\alpha_1\alpha_2\right)d_2d_3e^{ik(\alpha_2-\alpha_1)z}+2(\alpha_1^2+1)d_2d_4\\+\left(3-\frac{1}{\alpha_1^2}\right)d_3^2e^{-2ik\alpha_1z}+\left(\alpha_1^2-2\alpha_2^2+3-\alpha_1\alpha_2+\frac{3\alpha_2}{\alpha_1}\right)d_3d_4e^{-ik(\alpha_1+\alpha_2)z}+(\alpha_1^2-4\alpha_2^2+1)d_4^2e^{-2ik\alpha_2z}\end{matrix}\right]dz \tag{C.2}$$

$$I = \left(\begin{array}{c} \frac{3\alpha_1^2-1}{2\alpha_1^3} d_1^2 (e^{2ik\alpha_1 h} - 1) + \frac{\alpha_1^2 - 2\alpha_1\alpha_2 + 3}{\alpha_1} d_1 d_2 (e^{ik(\alpha_1+\alpha_2)h} - 1) + 2\left(1 + \frac{1}{\alpha_1^2}\right) d_1 d_3 ikh + \\ \frac{\alpha_1^2 + 2\alpha_1\alpha_2 + 3}{\alpha_1} d_1 d_4 (e^{ik(\alpha_1-\alpha_2)h} - 1) + \frac{\alpha_1^2 - 4\alpha_2^2 + 1}{2\alpha_2} d_2^2 (e^{2ik\alpha_2 h} - 1) + \frac{-\alpha_1^2 - 2\alpha_1\alpha_2 - 3}{\alpha_1} d_2 d_3 (e^{ik(\alpha_2-\alpha_1)h} - 1) + \\ 2(\alpha_1^2 + 1) d_2 d_4 ikh + \frac{1 - 3\alpha_1^2}{2\alpha_1^3} d_3^2 e^{-2ik\alpha_1 z} + \frac{2\alpha_1\alpha_2 - \alpha_1^2 - 3}{\alpha_1} d_3 d_4 (e^{-ik(\alpha_1+\alpha_2)h} - 1) + \frac{4\alpha_2^2 - \alpha_1^2 - 1}{2\alpha_2} d_4^2 (e^{-2ik\alpha_2 h} - 1) \end{array} \right) \tag{C.3}$$

$$\hat{I} = ik \int_{-\infty}^{0} \left[(2\hat{d}_1 e^{k\hat{\alpha}_1 z} + (2\hat{\alpha}_2^2 - \hat{\alpha}_1^2 + 1)\hat{d}_2 e^{k\hat{\alpha}_2 z})(\hat{d}_1 e^{k\hat{\alpha}_1 z} + \hat{d}_2 e^{k\hat{\alpha}_2 z}) + \left(\left(\hat{\alpha}_1 + \frac{1}{\hat{\alpha}_1}\right)\hat{d}_1 e^{k\hat{\alpha}_1 z} + 2\hat{\alpha}_2 \hat{d}_2 e^{k\hat{\alpha}_2 z} \right)\left(\frac{1}{\hat{\alpha}_1}\hat{d}_1 e^{k\hat{\alpha}_1 z} + \hat{\alpha}_2 \hat{d}_2 e^{k\hat{\alpha}_2 z} \right) \right] dz \tag{C.4}$$

$$\hat{I} = ik \int_{-\infty}^{0} \left[\left(3 + \frac{1}{\hat{\alpha}_1^2}\right)\hat{d}_1^2 e^{2k\hat{\alpha}_1 z} + \left(2\hat{\alpha}_2^2 - \hat{\alpha}_1^2 + 3 + \hat{\alpha}_1\hat{\alpha}_2 + \frac{3\hat{\alpha}_2}{\hat{\alpha}_1}\right)\hat{d}_1\hat{d}_2 e^{k(\hat{\alpha}_1+\hat{\alpha}_2)z} + (4\hat{\alpha}_2^2 - \hat{\alpha}_1^2 + 1)\hat{d}_2^2 e^{2k\hat{\alpha}_2 z} \right] dz \tag{C.5}$$

$$\hat{I} = i\left[\frac{3\hat{\alpha}_1^2 + 1}{2\hat{\alpha}_1^3}\hat{d}_1^2 + \frac{2\hat{\alpha}_1\hat{\alpha}_2 - \hat{\alpha}_1^2 + 3}{\hat{\alpha}_1}\hat{d}_1\hat{d}_2 + \frac{4\hat{\alpha}_2^2 - \hat{\alpha}_1^2 + 1}{2\hat{\alpha}_2}\hat{d}_2^2 \right] \tag{C.6}$$

References

[1] J.L. Rose, Ultrasonic Guided Waves in Solid Media, Cambridge University Press, 2014.
[2] A.H. Nayfeh, Wave Propagation in Layered Anisotropic Media: With Applications to Composites, Elsevier, 1995.
[3] J.D. Achenbach, Wave Propagation in Elastic Solids, North-Holland, Publishing Company, 1973.
[4] W.M. Ewing, W.S. Zardetzky, F. Press, Elastic waves in layered media, McGraw-Hill, 1957.
[5] K.F. Graff, Wave Motion in Elastic Solids, State University Press, Ohio, 1975.
[6] T. Kundu, Ultrasonic Nondestructive Evaluation: Engineering and Biological Material Characterization, CRC Press, 2003.
[7] B.A. Auld, Acoustic Fields and Waves in Solids, Wiley, 1973.
[8] J.D. Achenbach, S.P. Keshava, Free waves in a plate supported by a semi-infinite continuum, J. Appl. Mech. 34 (1967) 397–404.
[9] H.F. Tiersten, Elastic surface waves guided by thin films, J. Appl. Phys. 40 (1969) 770–789.
[10] P.C. Vinh, V.T.N. Anh, V.P. Thanh, Rayleigh waves in an isotropic elastic half-space coated by a thin isotropic elastic layer with smooth contact, Wave Motion (2013).
[11] P.C. Vinh, V.T. Ngoc Anh, Rayleigh waves in an orthotropic half-space coated by a thin orthotropic layer with sliding contact, Int. J. Eng. Sci. 75 (2014) 154–164.
[12] J.D. Achenbach, Reciprocity in Elastodynamics, Cambridge University Press, 2003.
[13] J.D. Achenbach, A.K. Gautesen, H. McMaken, Ray methods for waves in elastic solids: with applications to scattering by cracks, Pitman Advanced Pub. Program, 1982.
[14] A.T. De Hoop, Handbook of Radiation and Scattering of Waves: Acoustic Waves in Fluids, Elastic Waves in Solids, Electromagnetic Waves, Academic Press, 1995.
[15] O. Balogun, J.D. Achenbach, Surface waves generated by a line load on a half-space with depth-dependent properties, Wave Motion 50 (2013) 1063–1072.
[16] H. Phan, Y. Cho, J.D. Achenbach, Validity of the reciprocity approach for determination of surface wave motion, Ultrasonics 53 (2013) 665–671.
[17] H. Phan, Y. Cho, J.D. Achenbach, Verification of surface wave solutions obtained by the reciprocity theorem, Ultrasonics 54 (2014) 1891–1894.
[18] L.R.F. Rose, W.K. Chiu, N. Nadarajah, B.S. Vien, Using reciprocity to derive the far field displacements due to buried sources and scatterers, J. Acoust. Soc. Am. 142 (2017) 2979–2987.
[19] H. Phan, T.Q. Bui, H.T.L. Nguyen, C.V. Pham, Computation of interface wave motions by reciprocity considerations, Wave Motion 79 (2018) 10–22.
[20] S.S. Kulkarni, J.D. Achenbach, Application of the reciprocity theorem to determine line-load-generated surface waves on an inhomogeneous transversely isotropic half-space, Wave Motion 45 (2008) 350–360.
[21] A. Pau, D. Capecchi, F. Vestroni, Reciprocity principle for scattered fields from discontinuities in waveguides, Ultrasonics 55 (2015) 85–91.
[22] H. Phan, Y. Cho, J.D. Achenbach, Application of the reciprocity theorem to scattering of surface waves by a cavity, Int. J. Solids Struct. 50 (2013) 4080–4088.
[23] H. Phan, Y. Cho, W. Li, A theoretical approach to multiple scattering of surface waves by shallow cavities in a half-space, Ultrasonics 88 (2018) 16–25.
[24] H. Phan, Y. Cho, T. Ju, J.D. Achenbach, S. Krishnaswamy, B. Strom, A novel approach of using the elastodynamic reciprocity for guided wave problems, AIP Conf. Proc. 1511 (2013) 107–112.
[25] S. Hao, B.W. Strom, G. Gordon, S. Krishnaswamy, J.D. Achenbach, Scattering of the lowest lamb wave modes by a corrosion pit, Res. Nondestruct. Eval. 22 (2011) 208–230.
[26] E. Kausel, Fundamental Solutions in Elastodynamics: A Compendium, Cambridge University Press, Cambridge, 2006.